In vitro analysis of antigen induced T cell-monocyte conjugates by Imaging flow cytometry

Meseret Habtamu [1,2], Markos Abebe[2], Abraham Aseffa[2], Anne Margarita Dyrhol Riise[3,4,5], Anne Spurkland[1], Greger Abrahamsen[1]

[1]*Department of Molecular Medicine, Institute of Basic Medical Sciences, University of Oslo, Norway,* [2]*Armauer Hansen Research Institute, Addis Ababa, Ethiopia*

[3]*Department of Infectious Disease, Oslo University Hospital, N-0424 Oslo, Norway*

[4]*Institute of Clinical Medicine, Faculty of Medicine, University of Oslo, N-0424 Oslo, Norway*

[5]*Department of Clinical Science, Faculty of Medicine, University of Bergen, N-5020 Bergen, Norway*

Corresponding author:

Greger Abrahamsen, Institute of Basic Medical Sciences, University of Oslo, Pb 1105 Blindern, 0317 Oslo, Norway. Email: greger.abrahamsen@medisin.uio.no, Phone: +47 22851216

Abstract

There is a lack of suitable correlates of immune protection against *Mycobacterium tuberculosis* (*Mtb*) infection. T cells and monocytes play key roles in host immunity against *Mtb*. Thus, a method that allows assessing their interaction would contribute to the understanding of immune regulation in tuberculosis (TB). We have established imaging flow cytometer (IFC) based *in vitro* assay for the analysis of early events in T cell-monocyte interaction, upstream of cytokine production and T cell proliferation. This was achieved through short term stimulation of peripheral blood mononuclear cells (PBMC) from healthy Norwegian blood donors with *Mycobacterium bovis* Bacille Calmette-Guérin (BCG). In our assay, we examined the kinetics of BCG uptake by monocytes using fluorescently labeled BCG and T cell-monocyte interaction based on synapse formation (CD3/TCR polarization). Our results showed that BCG stimulation induced a gradual increase in the proportion of conjugated T cells displaying NF-κB translocation to the nucleus in a time dependent manner, with the highest frequency observed at 6 hours. We subsequently tested PBMC from a small cohort of active TB patients (n=7) and observed a similar BCG induced NF-κB translocation in T cells conjugated with monocytes. The method allowed for simultaneous evaluation of T cell-monocyte conjugates and T cell activation as measured by NF-κB translocation, following short-term challenge of human PBMC with BCG. Whether this novel approach could serve as a diagnostic or prognostic marker needs to be investigated using a wide array of *Mtb* specific antigens in a larger cohort of patients with different TB infection status.

Key Words:

Imaging Flow Cytometery, BCG, Monocyte, Conjugate, Nuclear factor κappa-B

1. Introduction

Prominent progress has been made in the fight against tuberculosis (TB) in the past decades. Yet, it is still among the leading infectious causes of morbidity and mortality worldwide with an estimated 10.4 million new cases and 1.8 million associated deaths in 2015 (WHO, 2016). The development of novel approaches for the control and elimination of TB is challenged by the lack of tools to better understand the mechanisms and outcome of the host-pathogen interaction.

T cell mediated immune response of the Th-1 type is widely regarded as protective against TB (Kaufmann, 2006). The Th-1 cytokine, interferon gamma (IFN-γ) is considered a key protective cytokine based on earlier studies, in both mice and humans, which showed that defects in the IFN-γ signaling pathways provoked higher susceptibility to *Mycobacterium tuberculosis* (*Mtb*) infection and severe disease (Cooper et al., 1993; Newport et al., 1996; Flynn et al., 2003). Thus, many *in vitro* studies have focused on determining the frequency of *Mtb* specific T cells secreting IFN-γ alone, in combination with other Th-1 cytokines; IL-2 and TNFα measuring their level of secretion, and extent of T cell proliferation as markers of protection (McShane et al., 2004; Beveridge et al., 2008; Hoft et al., 2008; Smith et al., 2016). On the other hand, studies have shown that cytokine levels do not necessarily correlate with protective immunity nor predict risk of progression to active TB disease (Pai et al., 2004; Elias et al., 2005; Majlessi et al., 2006; Mittrucker et al., 2007; Panteleev et al., 2017). Developing suitable assays for the evaluation of protective immunity, risk of disease progression or immunogenicity of a vaccine is a priority in TB research (Centis et al., 2017).

It has long been established that T cell activation requires direct interaction between T cell surface receptors (TCR) and cogent peptide-major histocompatibility complex (pMHC) on the surface of antigen presenting cells (APCs) such as monocytes, macrophages, dendritic cells and B cells (Rossjohn et al., 2015; Jakubzick et al., 2017). Efficient TCR and pMHC interaction triggers signaling from the TCR-CD3 complex. Together with signals from costimulatory molecules, this results in the reorganization of T cell cytoskeletal elements with polarization of TCR as well as other signaling molecules towards the contact site resulting in the formation of an immunological synapse (IS) (Grakoui et al., 1999). The IS formation ensured sustained intracellular signaling in T cells, which involves translocation of transcription factors from the

cytoplasm to the nucleus (Kane et al., 2000). Nuclear factor kappa-B (NF-κB) is a transcription factor that regulates various genes involved in the host immune response; including cell proliferation and cytokine production (review in (Lucas et al., 2004; Tripathi and Aggarwal, 2006)). In the resting state, NF-κB is localized in the cytoplasm and translocates to the nucleus upon activation, where it regulates gene transcription. It has been shown that these early events are among the factors that influence the quality of host immune response (Grakoui et al., 1999; Kane et al., 2002). Thus, assessing T cell-APC interactions and NF-κB nuclear translocation could be a better estimate in monitoring efficiency of immune response against TB, than measuring individual effector molecules.

Here we describe the use of imaging flow cytometer (IFC) to simultaneously evaluate T cell-monocyte conjugates and T cell activation as measured by NF-κB translocation, following short-term BCG challenge *in vitro.* We used PBMC from buffy coats of healthy Norwegian blood donors as well as from TB patients residing in Norway.

2. Materials and Methods

1.2.1 Antibodies, reagents and antigens:

Antibodies used include anti-CD3 (clone OKT3), anti-CD28 (clone CD28.2, Cat# 555725, BD Pharmingen), anti-CD3-FITC (clone UCHT1, Cat# 21620033, Immunotools), anti-CD14-APC (clone MEM-15, Cat# 21279146, Immunotools), anti-IFN-γ PerCP Cy-5.5 (Clone B27, Cat # 560704, BD biosciences), rabbit polyclonal IgG (C-20) anti-human NF-κB primary antibody (SC-372R, Santa Cruz Biotechnology), Alexa Fluor 594, goat anti-rabbit IgG (H+L) secondary antibody (Cat# R37117, Molecular Probes, Invitrogen). Fluorescent reagents include LIVE/DEAD Fixable Near-IR (Cat# L34976, Molecular Probes, Invitrogen), and DAPI nuclear stain (Cat# 00-4959-52, Thermo Fisher) and CellTrace Violet (CTV) (Cat# C34557, Molecular probes, Invitrogen). RPMI 1640 (Gibco, Life Technologies) complete medium supplemented with 10% fetal calf serum (FCS), 100 units/ml penicillin, 100 μg/ml streptomycin (all from GIBCOBRL®, Life Technologies™), 1M HEPES buffer solution (Gibco, Life Technologies), 100mM Sodium-pyruvate (Gibco, Life Technologies), MEM NEAA (100x) (Gibco, Life Technologies), 2-Mercaptoethanol (Sigma)), Mycobacterial antigens used include: PPD for *in vitro* use (Statens Serum Institute, Copenhagen, Denmark) and ds-Red fluorescent protein expressing BCG (strain Myc3305, provided by Dr. Brigitte Gicquel) (Abadie et al., 2005).

1.2.2 Cell isolation and culture

Peripheral blood mononuclear cells (PBMC) from buffy coats, Oslo University Hospital, Norway, were isolated in high numbers by density gradient using Lymph prep (Axis–shield PoC AS, Cat # 1114545, Oslo, Norway) according to the manufacturer's protocol, and cryopreserved at a final concentration of 10% DMSO and 20% FCS until analysis. Prior to experiments, PBMC were thawed, washed and re-suspended in RPMI 1640 complete medium supplemented with 10% FCS, and allowed to rest overnight at 37^0C and 5% CO_2. PBMC ($1x10^6$ cells/ mL) were then incubated at 37^oC and 5% CO_2 with ds-Red expressing BCG, at a final concentration of $3x10^6$ CFU/mL for 6 hrs. PBMC incubated in culture medium alone under the same conditions were used as unstimulated control. Cells were harvested after careful scraping and resuspension, and then transferred to microcentrifuge tubes for fluorochrome staining and acquired by IFC.

For the pilot experiment PBMC from treatment-naïve clinically and/or bacteriologically confirmed patients with active TB (n=7) were obtained from the Norwegian biobank for infectious diseases, Oslo University Hospital, Ulleval. The research biobank is approved by the Regional Ethics Committee (REK Helse-sør-øst 2008.173) and written informed consent was obtained from all participants prior to sample collection. The culture condition for cells from patients was similar to the buffy coats mentioned above.

1.2.3 *In vitro* T cell proliferation and IFN-γ releasing T cells

PBMCs were thawed and rested as described above and fluorescently labeled using CTV, according to the manufacturer's instructions. CTV labeled cells were re-suspended in complete media to a concentration of $1x10^6$ cells/mL, in the presence of IL-2 and cultured at 37^o C in a 5% CO_2 atmosphere with the following antibodies or antigens added: plate bound anti-CD3 (5 μg/ml) and anti-CD28 (1 μg/ml), PPD (10 μg/ml) or ds-Red BCG ($3x10^6$ CFU/ml).

Unstimulated PBMC were used to assess background proliferation. Cells were then harvested on days 0, 4, 5, 6 and fluorochrome stained. In the preparation of IFN-γ production assay, brefeldin A (Sigma-Aldrich) was added to the five day culture prior to harvest and incubated for 4 hours. Following anti-CD3 surface staining, cells were fixed and IFN-γ intracellular staining was performed. Stained cells were acquired with a FACSCantoII flow cytometer using FACS Diva software (BD Biosciences) to determine CTV dye dilution on proliferating T cells and IFN-γ releasing T cells. Data analysis was performed using FlowJo version 10.0 (Tree Star Inc.).

1.2.4 Imaging flow cytometry

Throughout the protocol, wide bore pipette tips (VWR) were used. Harvested cells were washed once with cold FACS buffer (2% FCS, 0.1% sodium azide in PBS). To block nonspecific binding, cells were incubated with 10% heat inactivated human serum in FACS buffer for 10 minutes on ice and surface stained with anti-CD3-FITC and anti-CD14-APC antibodies by incubating for 20 minutes on ice and in the dark.

For detection of intracellular NF-κB, cells were fixed in 2% paraformaldehyde for 10 minutes at room temperature and incubated with 0.1% Triton-X permeabilization buffer (Sigma, USA) for 5 minutes. Cells were then incubated with rabbit antihuman NF-κB primary antibody for 30

minutes followed by AF594 labeled goat anti-rabbit secondary antibody together with DAPI nuclear stain for 30 minutes on ice and in the dark. Single color controls were prepared from PBMC and used for compensation.

An Amnis Image stream MkII 12 channel system fitted with 4 lasers was used for acquisition (Amnis Corporation, Seattle, WA). All acquisitions were performed at 40x magnification on a low stream flow rate setting using INSPIRE software (Amnis Corporation). Up to 100,000 events were acquired from each sample. Images acquired include bright field (Channels 01 and 09), CD3-FITC (Ch-02), ds-Red BCG (Ch-03), NF-κB AF594 (Ch-04), DAPI (Ch-07), CD14-APC (Ch-11) and live-dead fixative (Ch-12). Cellular events were acquired by setting a gate using a scatter plot that allowed discriminating cells from speed beads, which were used as an internal calibrator for the machine. The gated cells were plotted as a histogram to exclude non-cellular images that are DAPI negative. Single color controls of 10,000 events were acquired for each color in every experiment with all relevant lasers "on" and with the bright-field illumination and scatter laser "off", to acquire spectral compensation samples.

1.2.5 Imaging flow cytometry data Analysis

The imaging flow cytometry data was analyzed using the IDEAS v6.1 software (Amnis Corporation, Seattle, WA). A compensation matrix was created using 'raw image files' of single color controls and the IDEAS compensation wizard. Events in camera focus were selected on the basis of 'Gradient RMS' feature. Following this, an 'Area' versus 'Aspect ratio' plot was used to identify cellular aggregates and single cells where single cells have higher aspect ratio while aggregates have lower aspect ratio (Ahmed et al., 2009). T cells and monocytes were defined within each image using individual "object masks" based on the respective florescence intensity of CD3 and CD14. Two cell conjugates were identified from the aggregates on the basis of low 'nuclear Aspect ratio' based on DAPI signal and two cell nuclear content. From the two cell nuclear content, those adjacent with one T cell were gated on the basis of high 'CD3 Aspect ratio intensity'. This subpopulation was further gated to identify subpopulation of one T cell conjugated with one monocyte based on high 'CD14 Aspect ratio intensity'. We used TCR/CD3 polarization at the interface between a T cell and conjugating monocyte as marker for IS formation (Ahmed et al., 2009). To define the synapse within a T cell-monocyte conjugate, 'interface' mask was generated within the conjugating T

cell. The T cell-monocyte conjugate subpopulation was further separated by plotting ds-Red BCG fluorescent signal in CD14+ cells gated as BCG positive (BCG+) or BCG negative (BCG-). In order to determine NF-κB nuclear translocation in T cells, a software generated 'morphology' mask based on the nuclear image was applied to the 'Similarity' feature comparing the intensities of NF-κB and nuclear (DAPI) image, as previously described (George et al., 2006) within the T cells.

1.2.6 Statistical analysis

The GraphPad Prism 6 (GraphPad Software, La Jolla, CA, USA, www.graphpad.com) data analysis software was used to do statistical comparisons, summarizations and data presentation. Non-parametric, two-tailed tests were used for all comparisons. Two-way analysis of variance was applied to comparisons with multiple time points. The Wilcoxon matched-pairs test was used for matched data sets while Mann-Whitney U test to determine mean differences between TB cases and the healthy control group. P-values $\leq 0{\cdot}05$ were considered statistically significant.

3. Results

1.3.1 Fluorescent labeled BCG induced T cell proliferation *in vitro:* In order to assess the ability of ds-Red expressing BCG to induce *in vitro* lymphocyte proliferation, PBMC from Norwegian healthy blood donors (n=6) were analyzed in a fluorescence dilution assay using CTV at different time points (days 0,4,5 and 6) as a bench mark for cellular immune response against tuberculosis (Magnani et al., 2000).

Overlays of representative histograms showing CD4+ T cells with CTV dye dilution (CTV^{Low} events) in response to BCG, PPD, anti-CD3/CD28 or unstimulated cells (UNS), at various time points are shown in ***Fig. 1A***. Proportion of proliferating CD4+ T cells in response to various stimulants at the indicated times are summarized in ***Fig. 1B*** as line graphs. Anti-CD3/CD28 stimulation, used as positive control, induced massive proliferation of CD4+ T cells after 4 days of incubation, and reached close to 100% by day 6. PPD and BCG stimulation resulted in on average 47% and 36% CTV^{Low} CD4+ T cells at day 6, respectively (***Fig. 1B***). In parallel, we also analyzed the Th-1 cytokine IFN-γ secretion, measured at day 5 (***Fig. 1C)***. We observed that PPD (positive control) and BCG stimulation induced IFN-γ production in 14% and 11% of CD4+ T cells, respectively (***Fig. 1 D***). Taken together, our data indicated that presence of ds-Red expressing BCG in the cell culture induced a T cell response. We thus proceeded using the ds-Red BCG for further investigation.

1.3.2 IFC allowed monitoring the kinetics of BCG uptake and T cell-monocyte conjugate formation: We used TCR/CD3 polarization at the interface between T cells and monocytes as marker for immune synapse formation and NF-κB nuclear translocation as downstream effect after treating PBMC from healthy blood donors with ds-Red BCG and analyzed by IFC (***Fig. 2A).*** In order to define the optimal culture condition allowing simultaneous assessment of T cell-monocyte conjugates and NF-κB translocation, BCG titration with concentration up to $4x10^6$ CFU/ml (***Supplementary Fig.1***) and kinetics experiment up to 24 hours (***Supplementary Fig. 2***) were performed. The results showed a decline in the frequency of T cell-monocyte conjugates as the concertation increases, which was considerable at the highest concentration (***Supplementary Fig. 1A).*** A similar effect was observed in the proportions of T cell-monocyte conjugates and CD14+ cells as incubation time extended (***Supplementary Fig. 2A and 2B***). Conversely, more NF-kB translocation was induced in T cells with increased BCG

concentration and incubation time. We thus limited further experiments to BCG concentration of $3x10^6$ CFU/ml, which we found optimal.

T cell-monocyte conjugates were identified as outlined in the gating strategy (***Fig. 2B)*** and described in detail in the methods section. Briefly, two cell conjugates were selected by their low aspect ratio of the nuclear images based on DAPI signal. Of the two cell conjugates subpopulation, events of one T cell engaged with one monocyte were identified by their high CD3 and CD14 aspect ratio plotted consecutively (***Fig. 2B vi, 2B vii and 2B viii)***. An image gallery is presented showing individual images and T cell-monocyte conjugates (***Fig. 3A***). Immunological synapse (IS) formation was determined by applying 'Interface mask' with TCR/CD3 polarization at the contact site between the two cells as shown in the image gallery (***Fig. 3A***, last column) and gated as in ***Fig. 3B***. Although there was a trend towards higher frequency of T cell-monocyte conjugates with polarized TCR/CD3 in BCG stimulated compared to unstimulated cells during the early hours of stimulation, it was terminated after 3 hour incubation (***Fig. 3C***). We also examined conjugates formed between T cell and BCG infected monocyte based on ds-Red fluorescent detection (***Fig. 3A***, upper panel*)* and gated in ***Fig. 3D*** and found that the frequency of T cells conjugated with BCG positive monocytes increase over time, from11% after 1 hour reaching to 25% after 6 hours (***Fig. 3E***).

1.3.3 NF-κB translocation in T cells increased with time following *in vitro* BCG stimulation: Having found that monocytes readily take up BCG (***Fig. 3***), we moved on to analyze its impact on T cell activation. Taking advantage of the capacity of IFC to monitor intracellular localization of fluorescently labeled molecules, we examined NF-κB nuclear translocation in T cells in response to BCG stimulation and the optimal time point for this was determined. Cells were probed with fluorescently labelled antibody to visualize NF-κB and stained with DAPI to visualize the nucleus. The NF-κB signal, the nuclear mask within the T cell along with their composite are presented in ***Fig. 4A***. We applied 'Similarity feature' to quantify the level of NF-κB nuclear localization based on correlation between the two images. Representative similarity plot histogram overlay of cells treated with BCG, PMA/ionomycin (positive control) and unstimulated cells (negative control) is presented to show how subpopulation of T cells with NF-κB translocation were identified (***Fig. 4B***). The proportion of T cells display NF-κB translocation increased over time in response to BCG stimulation. The

frequency of T cell conjugates displaying NF-κB nuclear translocation was an average of 4% at 1 hour and increased to 14% at 6 hours of incubation (***Fig. 4C***). Thus, for subsequent experiments, we considered the 6 hour incubation to be optimal for measuring T cell-monocyte conjugate formation and induced NF-κB nuclear translocation.

1.3.4 T cell-monocyte conjugate formation in active TB cases following *in vitro* BCG stimulation: The majority of Norwegian healthy blood donors have been BCG vaccinated as teenagers. However, the BCG vaccination status of the blood donors tested here was unknown. In order to assess whether *Mtb*-infected individuals respond differently to BCG in the IFC conjugate assay, we challenged PBMC from confirmed active treatment naïve TB patients (n=7) with BCG for 6 hours and compared this to the results obtained using PBMCs from healthy blood donors (n=6). Our data showed that there was no significant difference in the frequency of T cell-monocyte conjugates in response to BCG stimulation, neither in TB cases nor in healthy controls, compared to unstimulated control cells (***Fig. 5A***). In addition, no significant difference was observed among TB cases and healthy controls in the frequency of total BCG induced T cell-monocyte conjugates as well as the frequency of conjugates of T cell-BCG infected monocytes (***Fig. 5B*** and ***5C,*** respectively).

1.3.5 NF-κB nuclear translocation in T cells from active TB cases: Once we identified the T cell-monocyte conjugates in IFC analysis, we proceeded to consider T cell conjugates for NF-κB translocation analysis. Our data showed that the proportion of conjugates with NF-κB translocation was significantly higher upon BCG stimulation both in TB cases and healthy controls than in the spontaneously formed conjugates of unstimulated cells (UNS) (***Fig. 6A*** and ***6B***). A potential advantage of IFC evaluation of nuclear translocation of a cytosolic protein is the ability to detect and quantify this event in a heterogeneous population of cells at a single cell level or in the cell of interest interacting with another cell. When we compared NF-κB nuclear translocation in single T cells to T cells which were engaged in conjugate with monocytes, we observed that the proportion of T cells displaying NF-κB translocation was significantly higher in conjugated T cells than in single T cells both in active TB patients and in controls (***Fig. 6B***). Although we observed a trend towards a higher proportion of T cells conjugated with BCG infected monocytes and displaying NF-κB translocation in TB cases than

in healthy controls, this difference did not reach statistical significance in this limited number of tested individuals (***Fig. 6C***).

4. Discussion

The immune response against *MTb* is complex and involves innate and adaptive immune cells (Zuniga et al., 2012; Liu et al., 2017). Although studies have reported controversial findings, monitoring host immunity to TB mainly relies on assessing antigen induced T cell proliferation and cytokine secretion (Mittrucker et al., 2007; Fletcher et al., 2016; Sakai et al., 2016; Smith et al., 2016). Here we established an imaging flow cytometer (IFC) based *in vitro* assay to evaluate multiple parameters of the early events in T cell activation, upstream of IFN-γ production and T cell proliferation in primary human cells.

The IFC platform, used here, is being well recognized in its application to assess large numbers of rare events and for analyzing co-localization of intracellular molecules (McFarlin and Gary, 2017) and thus providing statistically robust results. In recent years, various applications of IFC have been reported in TB research; including assessment of phagocytosis, phagosome maturation and *Mtb* replication inside macrophage differentiated THP-1 cells (Johansson et al., 2015; Ranjbar et al., 2015).

Being interested in biological markers for susceptibility to TB, we set out to establish an IFC-method for analyzing the early steps of T cell response to TB antigens as a correlate of host immunity. If feasible, such a method could have the potential in providing information on T cell response not given by the currently available assays, such as lymphocytes proliferation, IFN-γ release assay or enumeration of antigen specific T cells using tetramer staining.

In our assay, we monitored T cell-monocyte interaction using TCR/CD3 polarization as a marker for synapse formation. Using the IFC based assay, we also monitored antigen induced NF-κB translocation in interacting T cells with an IS. We observed a clear effect of BCG stimulation in terms of higher frequency of NF-κB translocation in T cell conjugates compared to spontaneously formed conjugates in unstimulated cells, especially from three to six hour incubation. Although the effect we observed was significantly lower compared to that observed in T cells conjugated with monocytes, NF-κB translocation was also induced in single T cells that were exposed to BCG, though no difference was measured between patient cohorts. This finding could be explained by Toll-like receptor (TLR) mediated response, which has been reported be expressed in T cells and directly influence effector function upon exposure to bacterial products (Reynolds and Dong, 2013).

The main aim of this work was to establish the method itself using PBMC from healthy Norwegian blood donors, many of whom had previously been immunized with BCG, and thus were expected to harbor T cells responsive to BCG. After the method was established, we also tested a small number of active TB cases. Although we noticed a trend towards an increase in stimulation induced response in TB cases compared to Norwegian healthy controls, the number of individuals included here was too small for this difference to reach statistical significance.

IFC has previously been used to assess conjugates formed between T cells with anti-CD3 coated macrophages (Ahmed et al., 2009) or anti-CD3 coated beads (Burbach et al., 2008). Another group has established a method in defining immune synapse formed between purified CD4+ T cells and dendritic cells (Markey et al., 2015). Here, we established an IFC method to identify and analyze signaling events in antigen induced T cell-monocyte conjugates in PBMC based on TCR/CD3 polarization at the synapse. Overall, no significant difference was found in the proportions of T cell-monocyte conjugates between BCG stimulated and unstimulated cells. Although we observed an increase in conjugate formation at the early time points, we also experienced a gradual decline in the number of CD14+ cells over time upon BCG challenge (***Supplementary Fig. 3***), which potentially could affect the number of conjugates identified. A similar observation was reported by Shey and colleagues that *in vitro* BCG challenge lowers the frequency of CD14+ cell (monocytes) (Shey et al., 2012) where phagocytosis induced shedding from the cell surface, micropinocytosis and monocyte death has been reported as possible causes (Mollen et al., 2008; Webster et al., 2010).

To our knowledge, this is the first report on the use of PBMC from humans in an IFC based assay to monitor the interaction between antigen presenting cell and T cell in response to live pathogen challenge (ds-Red BCG). The use of primary cells from healthy donors and active TB patients without sorting particular cell population, or using any additional inducement in the culture system, has the added value of measuring antigen-induced effect with minimal external influence. Monocytes are relatively rare in the circulation, and manipulations to enrich for the number of monocytes including purification by sorting has been reported to cause phenotypic and functional alterations (Delirezh et al., 2013), which could possibly influence on the results.

In conclusion, we have established an IFC based method using heterogeneous cell population to monitor early signaling events in T cells following antigen stimulation leading to various

effector functions. The method allowed for simultaneous evaluation of T cell-monocyte conjugates and T cell activation as measured by NF-κB translocation, following short-term BCG challenge of PBMC samples. This high throughput setting could help to address issues related to tetramer staining in assessing antigen specific T cell sub-populations (Vollers and Stern, 2008; Rius et al., 2018). Characterizing various aspects of immune cell interaction, combined with the consequence on the responding effector cell, might be used to address the current challenge of identifying correlate immune biomarkers of protection in TB or evaluation of vaccine induced responses. To substantiate if this platform would be instrumental in the search for biomarkers of diagnostic and/or prognostic value; further investigation with a larger cohort including TB patients with active disease as well as latent infection will be required. Adding more parameters for identifying IS may help improve assay specificity and sensitivity, allowing for differentiation of TB immunity in clinical samples. Moreover, the issue of antigen specific response and loss of CD14+ signal on monocytes that we observed with BCG stimulation could be addressed by using fluorescently labeled *Mtb* antigens or peptides.

Acknowledgments

This study was supported by grants from grants from Johs Svanholms grant, Henrik Homans Mindes grant, University of Oslo, Quota scheme of the Norwegian State, and Armauer Hansen Research Institute (AHRI). AHRI receives core support from Norad, Sida and the government of Ethiopia. The ds-Red fluorescent BCG strain Myc3305 is the property of Institut Pasteur, 25 rue du Docteur Roux, Francd 75015.

Conflict of interest

The authors declare that there is no conflict of interest.

Reference

Abadie, V., Badell, E., Douillard, P., Ensergueix, D., Leenen, P.J., Tanguy, M., Fiette, L., Saeland, S., Gicquel, B. and Winter, N., 2005, Neutrophils rapidly migrate via lymphatics after Mycobacterium bovis BCG intradermal vaccination and shuttle live bacilli to the draining lymph nodes. Blood 106, 1843-50.

Ahmed, F., Friend, S., George, T.C., Barteneva, N. and Lieberman, J., 2009, Numbers matter: Quantitative and dynamic analysis of the formation of an immunological synapse using imaging flow cytometry. Journal of Immunological Methods 347, 79-86.

Beveridge, N.E., Fletcher, H.A., Hughes, J., Pathan, A.A., Scriba, T.J., Minassian, A., Sander, C.R., Whelan, K.T., Dockrell, H.M., Hill, A.V., Hanekom, W.A. and McShane, H., 2008, A comparison of IFNgamma detection methods used in tuberculosis vaccine trials. Tuberculosis (Edinb) 88, 631-40.

Burbach, B.J., Srivastava, R., Medeiros, R.B., Gorman, W.E., Peterson, E.J. and Shimizu, Y., 2008, Distinct Regulation of Integrin-Dependent T Cell Conjugate Formation and NF-κB Activation by the Adapter Protein ADAP. The Journal of Immunology 181, 4840.

Centis, R., D'Ambrosio, L., Zumla, A. and Migliori, G.B., 2017, Shifting from tuberculosis control to elimination: Where are we? What are the variables and limitations? Is it achievable? International Journal of Infectious Diseases 56, 30-33.

Cooper, A.M., Dalton, D.K., Stewart, T.A., Griffin, J., Russell, D. and Orme, I., 1993, Disseminated tuberculosis in interferon gamma gene-disrupted mice. The Journal of experimental medicine 178, 2243-2247.

Delirezh, N., Shojaeefar, E., Parvin, P. and Asadi, B., 2013, Comparison The Effects of Two Monocyte Isolation Methods, Plastic Adherence and Magnetic Activated Cell Sorting Methods, on Phagocytic Activity of Generated Dendritic Cells. Cell Journal (Yakhteh) 15, 218-223.

Elias, D., Akuffo, H. and Britton, S., 2005, PPD induced in vitro interferon gamma production is not a reliable correlate of protection against Mycobacterium tuberculosis. Transactions of the Royal Society of Tropical Medicine and Hygiene 99, 363-8.

Fletcher, H.A., Snowden, M.A., Landry, B., Rida, W., Satti, I., Harris, S.A., Matsumiya, M., Tanner, R., O'Shea, M.K., Dheenadhayalan, V., Bogardus, L., Stockdale, L., Marsay, L., Chomka, A., Harrington-Kandt, R., Manjaly-Thomas, Z.R., Naranbhai, V., Stylianou, E., Darboe, F., Penn-Nicholson, A., Nemes, E., Hatheril, M., Hussey, G., Mahomed, H., Tameris, M., McClain, J.B., Evans, T.G., Hanekom, W.A., Scriba, T.J. and McShane, H., 2016, T-cell activation is an immune correlate of risk in BCG vaccinated infants. Nature communications 7, 11290.

Flynn, J., Capuano, S., Croix, D., Pawar, S., Myers, A., Zinovik, A. and Klein, E., 2003, Non-human primates: a model for tuberculosis research. Tuberculosis 83, 116-118.

George, T.C., Fanning, S.L., Fitzgeral-Bocarsly, P., Medeiros, R.B., Highfill, S., Shimizu, Y., Hall, B.E., Frost, K., Basiji, D., Ortyn, W.E., Morrissey, P.J. and Lynch, D.H., 2006, Quantitative measurement of nuclear translocation events using similarity analysis of multispectral cellular images obtained in flow. Journal of Immunological Methods 311, 117-129.

Grakoui, A., Bromley, S.K., Sumen, C., Davis, M.M., Shaw, A.S., Allen, P.M. and Dustin, M.L., 1999, The immunological synapse: a molecular machine controlling T cell activation. Science (New York, N.Y.) 285, 221-7.

Hoft, D.F., Blazevic, A., Abate, G., Hanekom, W.A., Kaplan, G., Soler, J.H., Weichold, F., Geiter, L., Sadoff, J.C. and Horwitz, M.A., 2008, A new recombinant bacille Calmette-Guerin vaccine safely induces significantly enhanced tuberculosis-specific immunity in human volunteers. Journal of Infectious Diseases 198, 1491-1501.

Jakubzick, C.V., Randolph, G.J. and Henson, P.M., 2017, Monocyte differentiation and antigen-presenting functions. Nature reviews. Immunology 17, 349-362.
Johansson, J., Karlsson, A., Bylund, J. and Welin, A., 2015, Phagocyte interactions with Mycobacterium tuberculosis — Simultaneous analysis of phagocytosis, phagosome maturation and intracellular replication by imaging flow cytometry. Journal of Immunological Methods 427, 73-84.
Kane, L.P., Lin, J. and Weiss, A., 2000, Signal transduction by the TCR for antigen. Current opinion in immunology 12, 242-249.
Kane, L.P., Lin, J. and Weiss, A., 2002, It's all Rel-ative: NF-kappaB and CD28 costimulation of T-cell activation. Trends in immunology 23, 413-20.
Kaufmann, S.H., 2006, Envisioning future strategies for vaccination against tuberculosis. Nature Reviews Immunology 6, 699-704.
Liu, C.H., Liu, H. and Ge, B., 2017, Innate immunity in tuberculosis: host defense vs pathogen evasion. Cell Mol Immunol.
Lucas, P.C., McAllister-Lucas, L.M. and Nunez, G., 2004, NF-kappaB signaling in lymphocytes: a new cast of characters. Journal of cell science 117, 31-9.
Magnani, Z.I., Confetti, C., Besozzi, G., Codecasa, L.R., Panina-Bordignon, P., Lang, R., Rossi, G.A., Pardi, R. and Burastero, S.E., 2000, Circulating, Mycobacterium tuberculosis-specific lymphocytes from PPD skin test-negative patients with tuberculosis do not secrete interferon-gamma (IFN-γ) and lack the cutaneous lymphocyte antigen skin-selective homing receptor. Clinical and Experimental Immunology 119, 99-106.
Majlessi, L., Simsova, M., Jarvis, Z., Brodin, P., Rojas, M.-J., Bauche, C., Nouzé, C., Ladant, D., Cole, S.T., Sebo, P. and Leclerc, C., 2006, An Increase in Antimycobacterial Th1-Cell Responses by Prime-Boost Protocols of Immunization Does Not Enhance Protection against Tuberculosis. Infection and Immunity 74, 2128-2137.
Markey, K.A., Gartlan, K.H., Kuns, R.D., MacDonald, K.P.A. and Hill, G.R., 2015, Imaging the immunological synapse between dendritic cells and T cells. Journal of Immunological Methods 423, 40-44.
McFarlin, B.K. and Gary, M.A., 2017, Flow cytometry what you see matters: Enhanced clinical detection using image-based flow cytometry. Methods 112, 1-8.
McShane, H., Pathan, A.A., Sander, C.R., Keating, S.M., Gilbert, S.C., Huygen, K., Fletcher, H.A. and Hill, A.V., 2004, Recombinant modified vaccinia virus Ankara expressing antigen 85A boosts BCG-primed and naturally acquired antimycobacterial immunity in humans. Nature medicine 10, 1240-1244.
Mittrucker, H.W., Steinhoff, U., Kohler, A., Krause, M., Lazar, D., Mex, P., Miekley, D. and Kaufmann, S.H., 2007, Poor correlation between BCG vaccination-induced T cell responses and protection against tuberculosis. Proceedings of the National Academy of Sciences of the United States of America 104, 12434-9.
Mollen, K.P., Gribar, S.C., Anand, R.J., Kaczorowski, D.J., Kohler, J.W., Branca, M.F., Dubowski, T.D., Sodhi, C.P. and Hackam, D.J., 2008, Increased expression and internalization of the endotoxin co-receptor CD14 in enterocytes occurs as an early event in the development of experimental necrotizing enterocolitis. Journal of pediatric surgery 43, 1175-1181.
Newport, M.J., Huxley, C.M., Huston, S., Hawrylowicz, C.M., Oostra, B.A., Williamson, R. and Levin, M., 1996, A mutation in the interferon-γ–receptor gene and susceptibility to mycobacterial infection. New England Journal of Medicine 335, 1941-1949.
Pai, M., Riley, L.W. and Colford, J.M., 2004, Interferon-γ assays in the immunodiagnosis of tuberculosis: a systematic review. The Lancet infectious diseases 4, 761-776.

Panteleev, A.V., Nikitina, I.Y., Burmistrova, I.A., Kosmiadi, G.A., Radaeva, T.V., Amansahedov, R.B., Sadikov, P.V., Serdyuk, Y.V., Larionova, E.E., Bagdasarian, T.R., Chernousova, L.N., Ganusov, V.V. and Lyadova, I.V., 2017, Severe Tuberculosis in Humans Correlates Best with Neutrophil Abundance and Lymphocyte Deficiency and Does Not Correlate with Antigen-Specific CD4 T-Cell Response. Frontiers in Immunology 8.

Ranjbar, S., Haridas, V., Jasenosky, L.D., Falvo, J.V. and Goldfeld, A.E., 2015, A Role for IFITM Proteins in Restriction of Mycobacterium tuberculosis Infection. Cell reports 13, 874-83.

Reynolds, J.M. and Dong, C., 2013, Toll-like receptor regulation of effector T lymphocyte function. Trends in immunology 34, 511-519.

Rius, C., Attaf, M., Tungatt, K., Bianchi, V., Legut, M., Bovay, A., Donia, M., thor Straten, P., Peakman, M., Svane, I.M., Ott, S., Connor, T., Szomolay, B., Dolton, G. and Sewell, A.K., 2018, Peptide–MHC Class I Tetramers Can Fail To Detect Relevant Functional T Cell Clonotypes and Underestimate Antigen-Reactive T Cell Populations. The Journal of Immunology 200, 2263.

Rossjohn, J., Gras, S., Miles, J.J., Turner, S.J., Godfrey, D.I. and McCluskey, J., 2015, T Cell Antigen Receptor Recognition of Antigen-Presenting Molecules. Annual Review of Immunology 33, 169-200.

Sakai, S., Kauffman, K.D., Sallin, M.A., Sharpe, A.H., Young, H.A., Ganusov, V.V. and Barber, D.L., 2016, CD4 T Cell-Derived IFN-gamma Plays a Minimal Role in Control of Pulmonary Mycobacterium tuberculosis Infection and Must Be Actively Repressed by PD-1 to Prevent Lethal Disease. PLoS pathogens 12, e1005667.

Shey, M.S., Hughes, E.J., de Kock, M., Barnard, C., Stone, L., Kollmann, T.R., Hanekom, W.A. and Scriba, T.J., 2012, Optimization of a whole blood intracellular cytokine assay for measuring innate cell responses to mycobacteria. J Immunol Methods 376, 79-88.

Smith, S.G., Zelmer, A., Blitz, R., Fletcher, H.A. and Dockrell, H.M., 2016, Polyfunctional CD4 T-cells correlate with in vitro mycobacterial growth inhibition following Mycobacterium bovis BCG-vaccination of infants. Vaccine 34, 5298-5305.

Tripathi, P. and Aggarwal, A., 2006, NF-kB transcription factor: a key player in the generation of immune response. CURRENT SCIENCE-BANGALORE- 90, 519.

Vollers, S.S. and Stern, L.J., 2008, Class II major histocompatibility complex tetramer staining: progress, problems, and prospects. Immunology 123, 305-13.

Webster, S.J., Daigneault, M., Bewley, M.A., Preston, J.A., Marriott, H.M., Walmsley, S.R., Read, R.C., Whyte, M.K. and Dockrell, D.H., 2010, Distinct cell death programs in monocytes regulate innate responses following challenge with common causes of invasive bacterial disease. Journal of immunology (Baltimore, Md. : 1950) 185, 2968-79.

WHO 2016. Global Tuberculosis Report. World Health Organization.

Zuniga, J., Torres-Garcia, D., Santos-Mendoza, T., Rodriguez-Reyna, T.S., Granados, J. and Yunis, E.J., 2012, Cellular and humoral mechanisms involved in the control of tuberculosis. Clinical & developmental immunology 2012, 193923.

Figure Legends

Fig 1: Antigen induced lymphocyte proliferation and IFN-γ production *in vitro:* PBMC from healthy blood donors (n=6) labelled with CellTrace Violet (CTV) were cultured for 6 days in the presence of PPD, ds-Red BCG, anti-CD3/CD28 or media alone (UNS). Cells were harvested at various time points, fluorochrome stained and analyzed by flow cytometer for CTV dilution. (**A**) Representative histogram overlays; 0, 4, 5 and 6 days *in vitro* are shown here with the gate indicating CTV_{Low} CD4+ events. (**B**) Frequency of CD4+ T cells with CTV dye dilution (CTV_{Low} events) in response to anti-CD3/CD28 (dotted line with triangles), PPD (dashed line with circles), ds-Red BCG (solid line with squares), or UNS (gray line with diamond) at days 0, 4, 5 & 6. Error bars show mean ± SD. (**C**) Representative dot plots of IFN-γ secreting CD4+ T cell. (**D**) Proportion of IFN-γ secreting CD4+ T cells in response to PPD (circles), ds-Red BCG (squares), anti-CD3/CD28 (inverted triangle) or UNS (triangles). Horizontal bars indicate median values.

Fig 2: Assay outline and gating strategy applied to identify single cells, conjugates and NF-κB translocation in T cells: **(A)** Schematic diagram summarizing cell preparation and analysis. PBMC from healthy donors (n=6) were incubated with ds-Red BCG (BCG) for 6 hours, fluorochrome stained and analyzed by IFC. **(B)** Cells in camera focus were selected from all events on the basis of gradient RMS of the bright field image (i). Single cells and cellular aggregates were identified by plotting 'Area' versus 'Aspect ratio' in which events with higher 'Aspect ratio' are likely to be single cells while those with lower 'Aspect ratio' are aggregates (ii). Live cells were identified from the single cell sub-population based on live/dead stain (iii). Single T cells and monocytes were plotted from live cell sub-population based on CD3 and CD14 fluorescent intensities in Ch-2 and Ch-11, respectively (iv). As for single cells, live cells from cellular aggregates were identified on the basis of live/dead stain (v). Two-cell nuclei were defined by plotting 'Intensity of DAPI' against 'Aspect ratio intensity of DAPI' from the aggregates where those with low 'Aspect ratio' are gated (vi). From the subpopulation of cells with two nuclei, those with one T cell were identified by plotting 'Intensity of Ch-2 (CD3_FITC)' against 'Aspect ratio intensity of Ch-2' where those with high 'aspect ratio intensity' are gated (vii). Conjugates with one T cell and one monocyte were identified by

plotting “intensity of Ch-11” (CD14_APC) against “Aspect ratio intensity of Ch-11” (viii), events with high ‘Aspect ratio intensity’ are gated as population of interest.

Fig 3: Kinetics of BCG uptake and T cell-monocyte conjugate formation. (**A**) Image gallery, from left to right; showing bright field (BF) images in the first column, followed by T cells and monocytes based on CD3_FITC (green), and CD14_APC (red) fluorescent signal intensities, respectively. Masked images are shown in the right hand side of the respective images. BCG infected monocytes were identified based on detection of ds-Red fluorescent signal within CD14+ cells. Merged imageries are shown as; T cell conjugated with ds-Red BCG positive monocyte (upper panel) or monocyte with no ds-Red BCG (lower panel). Last column presents DAPI images of T cell-monocyte conjugates with ‘interface’ mask. (**B**) Representative histogram overlay for TCR/CD3 polarization at 6 hours incubation of cells with BCG (red) or left unstimulated (UNS) (black). (**C**) Frequency of T cell-monocyte conjugates following BCG challenge (solid line) or UNS (dashed line), monitored for 6 subsequent time points in an hour interval. (**D**) Representative histograms defining BCG positive and BCG negative T cell-monocyte conjugates. (**E)**, Proportion of ds-Red BCG positive conjugates relative to all T cell-monocyte conjugates in BCG stimulated cells, analyzed sequentially for 6 time points. Line graphs represent mean values from 6 healthy blood donors and error bars show mean $\pm$ SD.

Fig 4: Kinetics of BCG induced NF-κB nuclear translocation in T cells: PBMC from healthy donors (n=6) were co-cultured with ds-Red BCG and analyzed as outlined in in Fig 2. (**A**). A gallery showing bright field (BF) images of two cell conjugates in the first column followed by T cell-monocyte conjugates as CD3+ (green)-CD14+ (red), ds-Red BCG in the third column followed by NF-κB (golden brown) followed by DAPI mask. The last two columns present nuclear mask within T cell and merged images determining NF-κB nuclear localization: ‘high similarity’ between fluorecent intensities of NF-κB and DAPI images represents translocation (top panel) and ‘low similarity’ is for no translocation (bottom panel). The first and third raws represnt T cells conjugated with BCG infected mocoytes while second and fourth raws show no BCG. (**B**) Representative histogram overlay for NF-κB translocation in T cells in response to BCG (black), PMA/ ionomycin (red) or UNS (gray) at 6 hour incubation. (**C**) Proportion of NF-κB translocation in T cell conjugates at the indicated time

points. Solid lines with circles represent BCG stimulated cells while dashed lines with squares indicated UNS. Line graphs represent mean values from 6 healthy blood donors. Error bars show mean ± SD. Statistical significance was determined by two-way analysis of variance. $^{*}P<0.05$, $^{***}P<0.001$, $^{****}P<0.0001$.

Fig 5: T cell-monocyte conjugates in active TB cases and healthy controls: T cell-monocyte conjugates were analyzed in confirmed TB cases (n=7) and healthy controls (HC) (n=6) following PBMC challenged for 6 hours with BCG or media (UNS). (**A**) Frequency of T cell-monocyte conjugates with synapse relative to all T cell-monocyte conjugates in BCG stimulated and UNS pairs of TB cases and healthy contols. (**B**) Frequency of T cell-monocyte conjugates with synapse relative to all T cell-monocyte conjugates in TB cases and healthy controls upon BCG stimulation. (**C**) Proportion of ds-Red BCG positive T cell-monocyte conjugates in TB cases and healthy controls. Median values are indicated by horizontal lines (**B** and **C**).

Fig 6: NF-κB nuclear translocation in T cells of active TB cases and healthy controls: PBMC from confirmed TB cases (n=7) and healthy controls (HC) (n=6) were incubated for 6 hours. (**A**) Frequency of T cell conjugates displaying NF-κB translocation in response to BCG stimulation in active TB cases and HC relative to all T cell-monocyte conjugates. (**B**) Proportion of single T cells (s-CD3; squares) compared with T cell conjugates (c-CD3; circles) displaying NF-κB translocation in PBMC from active TB cases and HC in response to BCG stimulation. **(C)** Frequency of BCG positive (BCG+) T cell conjugates displaying NF-κB translocation in cells from active TB cases and HC. Horizontal lines (**B** and **C**) indicate median values. Wilcoxon matched-pairs signed rank test was used to assess changes after stimulation and Mann-Whitney test was used to compare median differences between TB cases and HC, $^{*}P<0.05$.

Figure 1

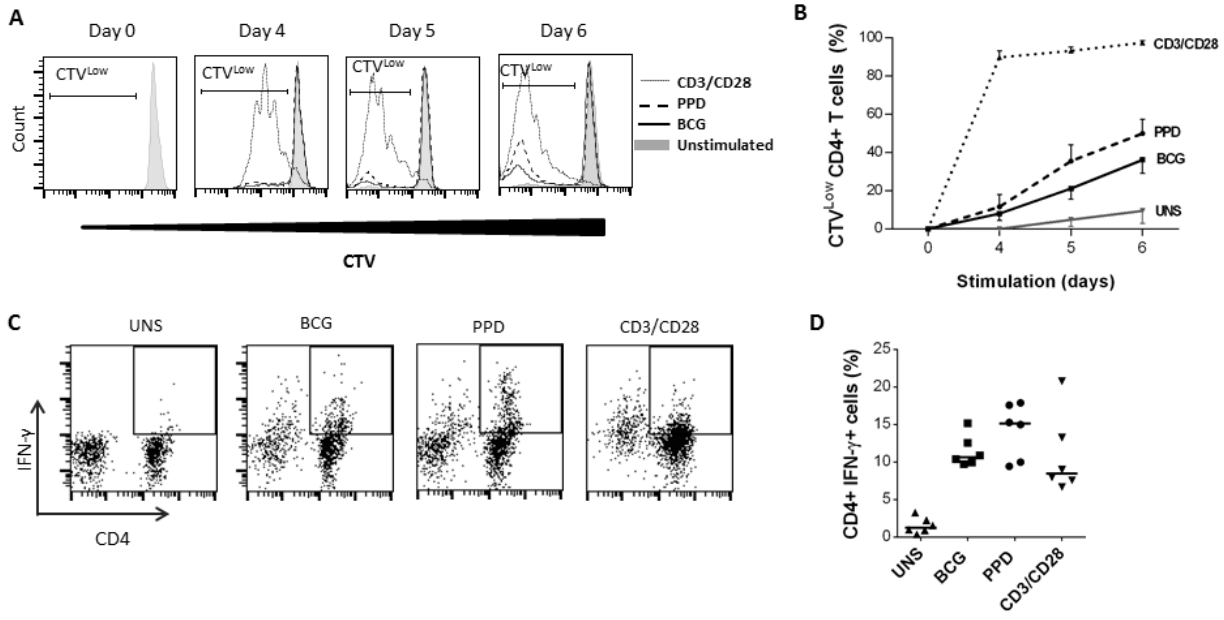
A
Day 0
Day 4
Day 5
Day 6
CTV^Low
Count
CD3/CD28
PPD
BCG
Unstimulated
CTV
B
CTV^Low CD4+ T cells (%)
CD3/CD28
PPD
BCG
UNS
Stimulation (days)
C
UNS
BCG
PPD
CD3/CD28
IFN-γ
CD4
D
CD4+ IFN-γ+ cells (%)
UNS
BCG
PPD
CD3/CD28

Figure 2

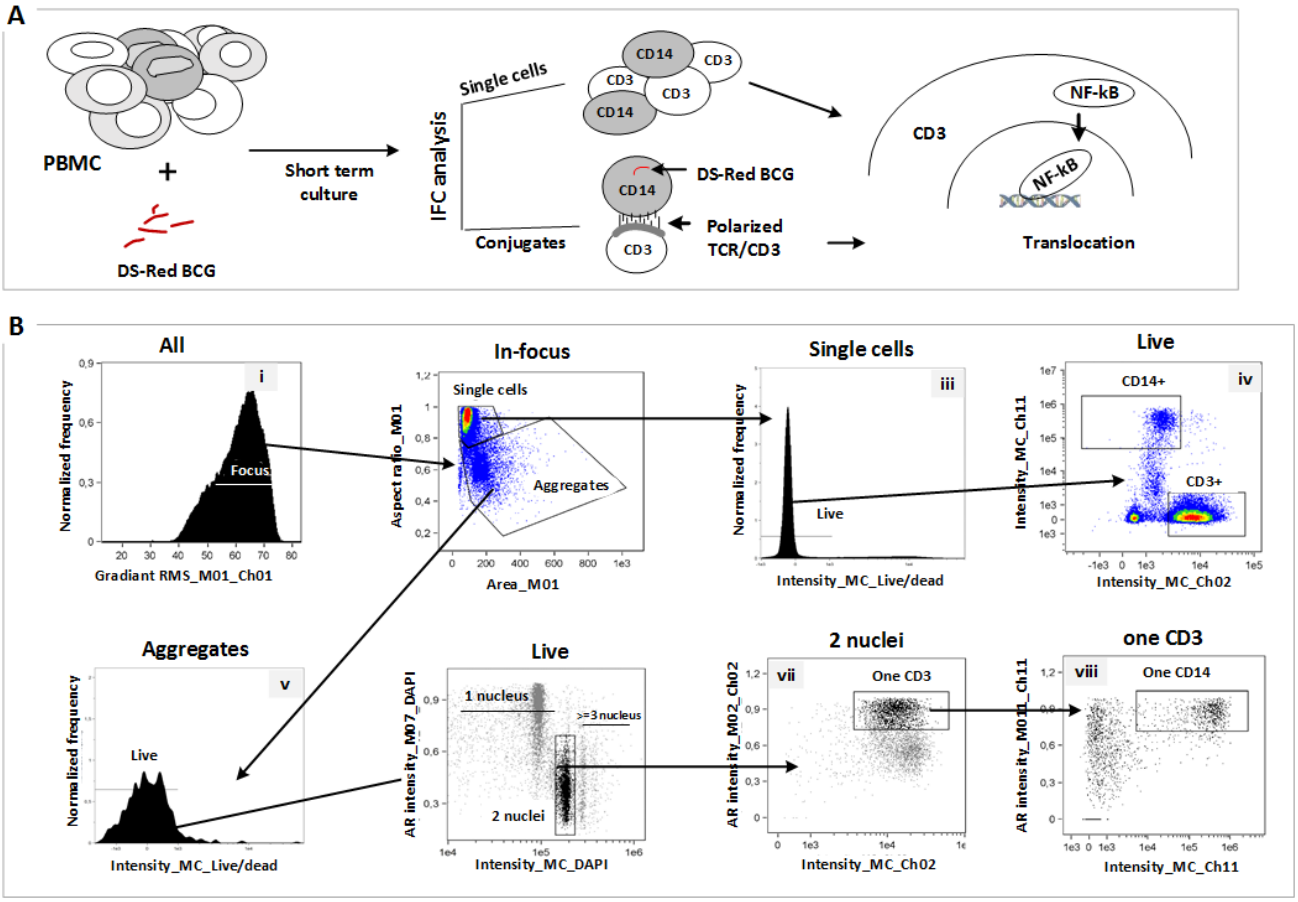
A
PBMC
+
DS-Red BCG
Short term culture
IFC analysis
Single cells
Conjugates
CD14
CD3
DS-Red BCG
Polarized TCR/CD3
NF-kB
Translocation
B
All
In-focus
Single cells
Live
Aggregates
2 nuclei
one CD3
Normalized frequency
Gradiant RMS_M01_Ch01
Focus
Aspect ratio_M01
Area_M01
Aggregates
Intensity_MC_Live/dead
CD14+
CD3+
Intensity_MC_Ch11
Intensity_MC_Ch02
AR intensity_M07_DAPI
1 nucleus
>=3 nucleus
2 nuclei
Intensity_MC_DAPI
One CD3
One CD14

Figure 3

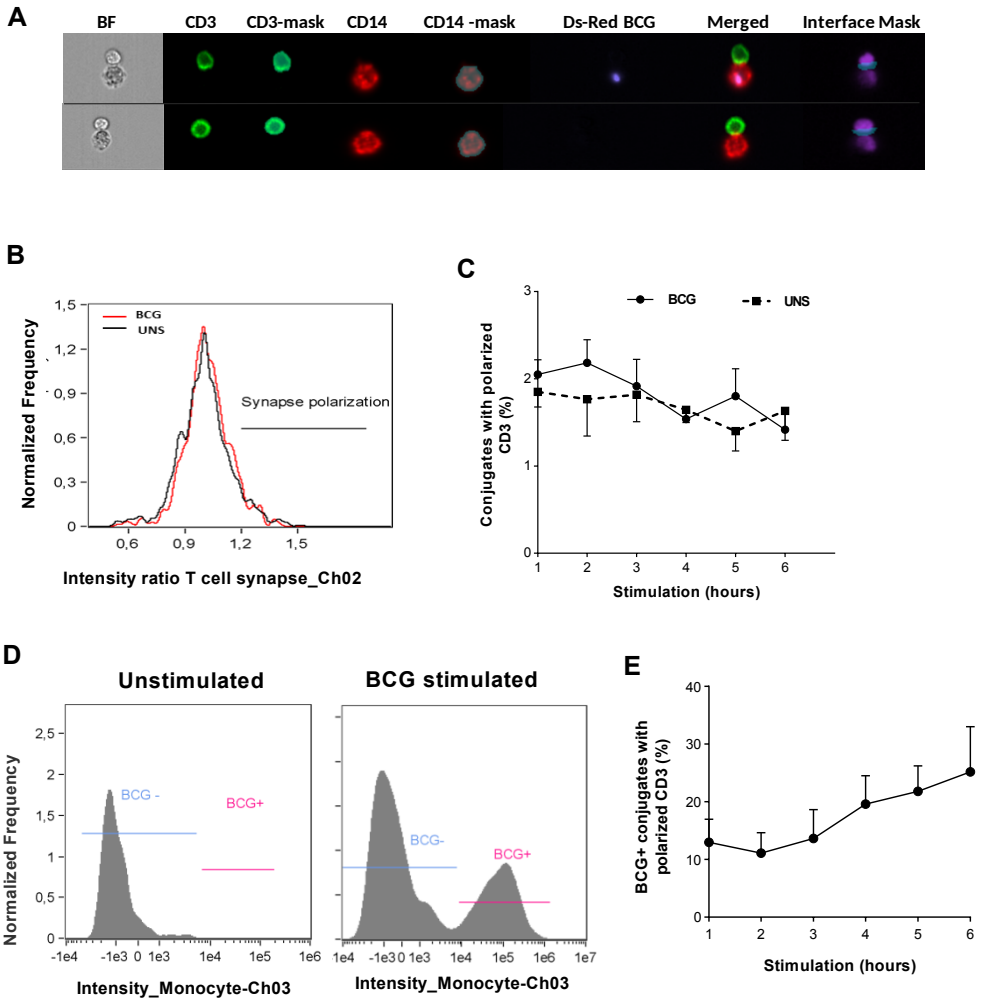
A
BF
CD3
CD3-mask
CD14
CD14 -mask
Ds-Red BCG
Merged
Interface Mask
B
Normalized Frequency
BCG
UNS
Synapse polarization
Intensity ratio T cell synapse_Ch02
C
Conjugates with polarized CD3 (%)
BCG
UNS
Stimulation (hours)
D
Unstimulated
BCG stimulated
Normalized Frequency
BCG -
BCG+
BCG-
BCG+
Intensity_Monocyte-Ch03
Intensity_Monocyte-Ch03
E
BCG+ conjugates with polarized CD3 (%)
Stimulation (hours)

Figure 4

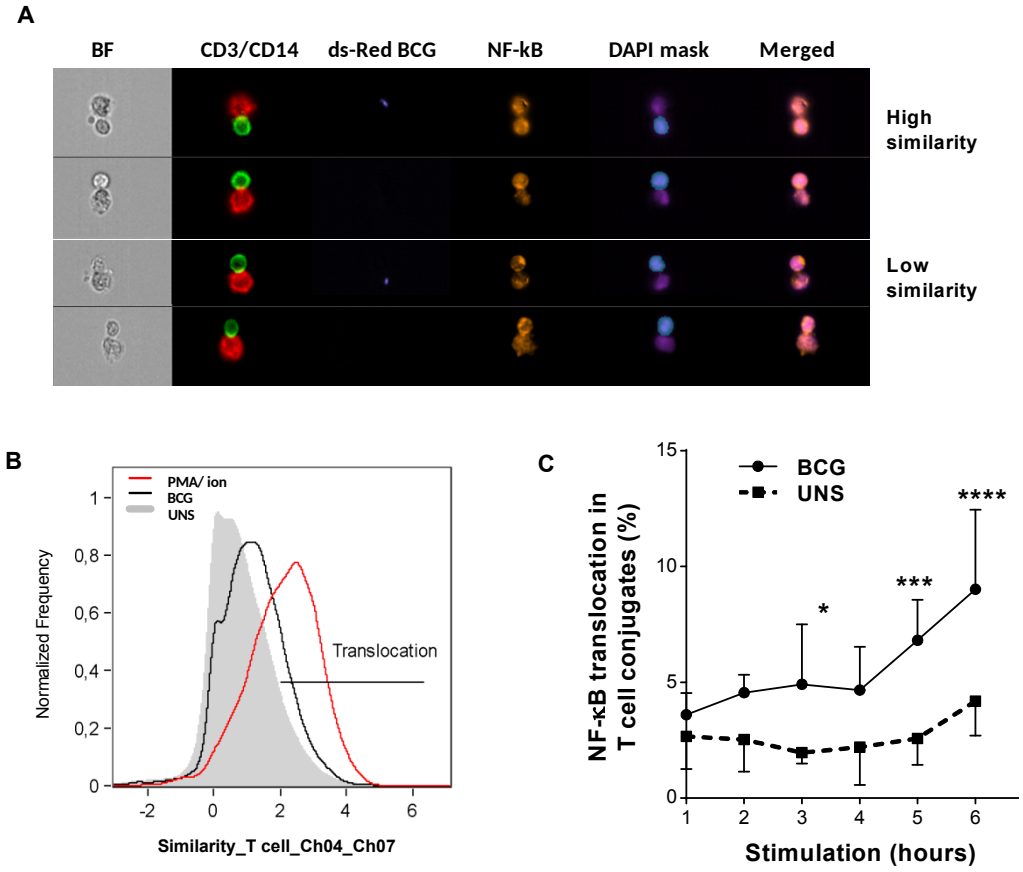
A
BF
CD3/CD14
ds-Red BCG
NF-kB
DAPI mask
Merged
High similarity
Low similarity
B
PMA/ ion
BCG
UNS
Normalized Frequency
Translocation
Similarity_T cell_Ch04_Ch07
C
BCG
UNS
NF-κB translocation in T cell conjugates (%)
Stimulation (hours)
*
***
****

Figure 5

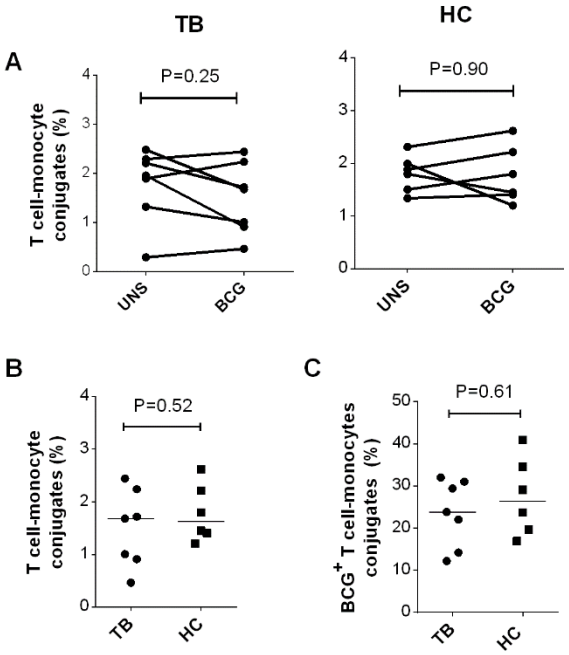
TB
HC
A
P=0.25
P=0.90
T cell-monocyte conjugates (%)
UNS
BCG
B
P=0.52
C
P=0.61
BCG+ T cell-monocytes conjugates (%)
TB
HC

Figure 6

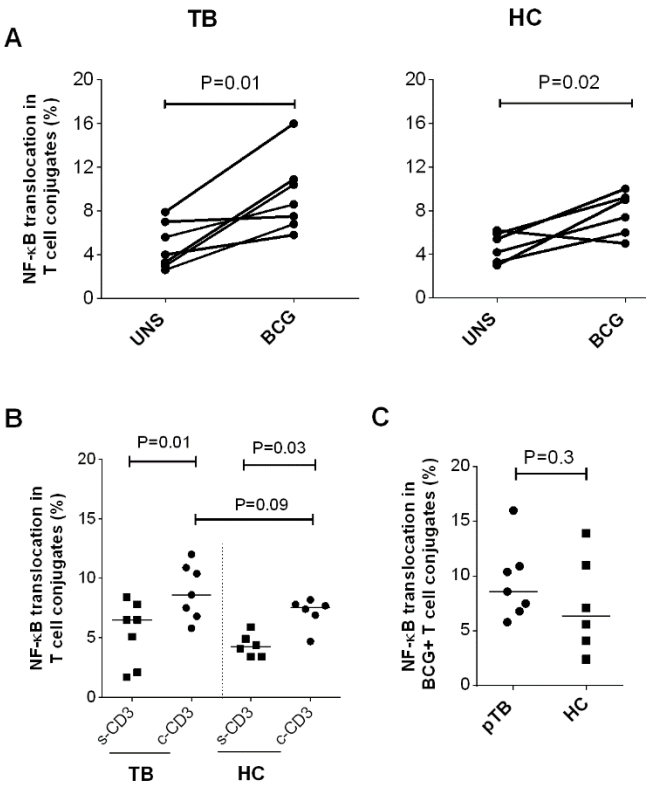
A
TB
HC
P=0.01
P=0.02
NF-κB translocation in T cell conjugates (%)
UNS
BCG
B
P=0.01
P=0.03
P=0.09
s-CD3
c-CD3
TB
HC
C
P=0.3
NF-κB translocation in BCG+ T cell conjugates (%)
pTB
HC

Supplementary Fig. 1: ds-Red BCG titration for T cell-monocyte conjugate and NF-kB translocation analysis: Healthy donor PBMC were co-cultured with BCG at various concentrations for 6 hours. Cells were harvested, fluorochrome stained and the following parameters were assessed by IFC. Frequency of T cell-monocyte conjugates (**A**), T cell conjugates displaying NF-κB translocation (**B**) and single T cells displaying NF-κB translocation (**C**). Bar graphs represent samples from 2 healthy blood donors. Error bars show mean ± SD.

Supplementary Fig. 2: Time kinetics of ds-Red BCG induced T cell monocyte interaction: Healthy donor PBMC were co-cultured with $3x10^6$ CFU/ml ds-Red BCG (BCG) or media (UNS) for 24 hours. Cells were harvested at 1, 6 and 24 hours, fluorochrome stained and the following parameters were assessed by IFC. Single CD14+ cells (**A**), T cell-monocyte conjugates (**B**), NF-κB nuclear translocation in T cell conjugates (**C**) and NF-κB translocation in all T cells (**D**) at the indicated time points. Black bars represent BCG stimulated sample while gray bars indicate unstimulated samples (UNS). Bar graphs represent samples from 2 healthy blood donors. Error bars show mean ± SD.

Supplementary Fig. 3: Proportions of T cells and monocytes following BCG stimulation: Healthy donor PBMC were co-cultured with ds-Red BCG (BCG) or media (UNS). Cells were harvested every hour for 6 consecutive time points fluorochrome stained and T cells and monocytes were asses by IFC. Frequencies single CD14+ cells (**A**) and single CD3+ cells (**B)** at the indicated time points. Solid lines with circles represet BCG stimulation and dashed lines with squares represent unstimulated samples. Line graphs represent samples from 6 healthy blood donors. Error bars show mean ± SD.

Supplementary figure 1

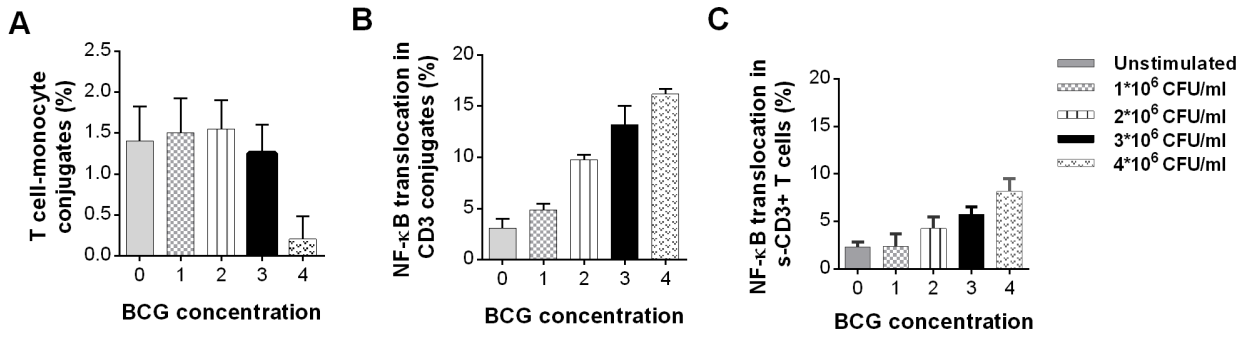

Supplementary figure 2

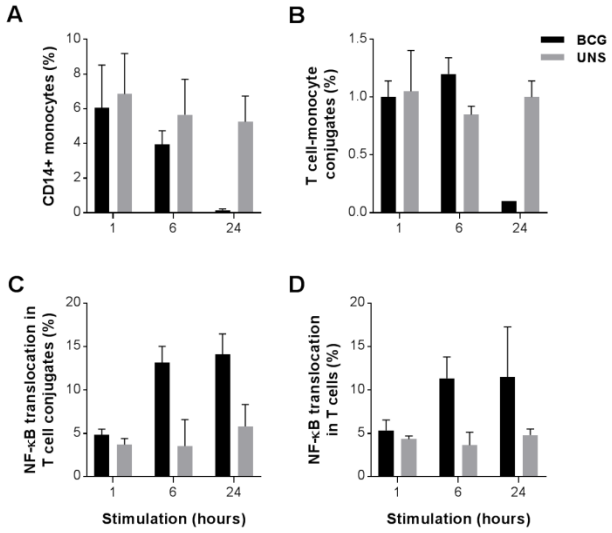

Supplementary figure 3